

## Correlated d0 ferromagnetism and photoluminescence in undoped ZnO nanowires

Guozhong Xing, Dandan Wang, Jiabao Yi, Lili Yang, Ming Gao et al.

Citation: *Appl. Phys. Lett.* **96**, 112511 (2010); doi: 10.1063/1.3340930

View online: <http://dx.doi.org/10.1063/1.3340930>

View Table of Contents: <http://apl.aip.org/resource/1/APPLAB/v96/i11>

Published by the [American Institute of Physics](#).

---

### Additional information on Appl. Phys. Lett.

Journal Homepage: <http://apl.aip.org/>

Journal Information: [http://apl.aip.org/about/about\\_the\\_journal](http://apl.aip.org/about/about_the_journal)

Top downloads: [http://apl.aip.org/features/most\\_downloaded](http://apl.aip.org/features/most_downloaded)

Information for Authors: <http://apl.aip.org/authors>

## ADVERTISEMENT



**HAVE YOU HEARD?**

Employers hiring scientists  
and engineers trust  
**physicstodayJOBS**



<http://careers.physicstoday.org/post.cfm>

# Correlated $d^0$ ferromagnetism and photoluminescence in undoped ZnO nanowires

Guozhong Xing,<sup>1</sup> Dandan Wang,<sup>1,2</sup> Jiabao Yi,<sup>3</sup> Lili Yang,<sup>4,5</sup> Ming Gao,<sup>4</sup> Mi He,<sup>1</sup> Jinghai Yang,<sup>4</sup> Jun Ding,<sup>3</sup> Tze Chien Sum,<sup>1</sup> and Tom Wu<sup>1,a)</sup>

<sup>1</sup>Division of Physics and Applied Physics, School of Physical and Mathematical Sciences, Nanyang Technological University, Singapore 637371

<sup>2</sup>Key Laboratory of Excited State Processes, Changchun Institute of Optics, Fine Mechanics and Physics, Chinese Academy of Sciences, Changchun 130033, and Graduate School of the Chinese Academy of Sciences, Beijing 100049, People's Republic of China

<sup>3</sup>Department of Materials Science and Engineering, National University of Singapore, Singapore 119260

<sup>4</sup>Institute of Condensed Matter Physics, Jilin Normal University, Siping 136000, People's Republic of China

<sup>5</sup>Department of Science and Technology, Linköping University, Campus Norrköping, SE-601 74 Norrköping, Sweden

(Received 15 December 2009; accepted 8 February 2010; published online 19 March 2010)

We report the correlated  $d^0$  ferromagnetism and photoluminescence in undoped single-crystalline ZnO nanowires synthesized by using a vapor transport method. We systematically tune the oxygen deficiency in the ZnO nanowires from 4% to 20% by adjusting the growth conditions, i.e., selecting different catalyst (Au or Ag) and varying the growth temperature. Our study suggests that oxygen vacancies induce characteristic photoluminescence and significantly boost the room-temperature ferromagnetism. Such undoped ZnO nanowires with tunable magnetic and optical properties are promising to find applications in multifunctional spintronic and photonic nanodevices. © 2010 American Institute of Physics. [doi:10.1063/1.3340930]

Wide band gap diluted magnetic semiconductors have gained much attention recently as a promising route to realize semiconductor-based spintronics.<sup>1</sup> ZnO posits as a prominent player, boasting a large exciton binding energy (60 meV) at room-temperature (RT) and many applications in optoelectronics and transparent electronics.<sup>2</sup> Recently, room-temperature ferromagnetism (RTFM) has been reported in ZnO doped with transition metals such as Mn, Co, and Cu, which makes ZnO promising for spintronics applications.<sup>3–5</sup> However, besides the issues of stability and reproducibility, it remains controversial whether RTFM is intrinsic or due to extrinsic origins such as metal clusters and precipitates of impurity phases. Adding to these existing literatures, there have been a few notable reports on RTFM in undoped ZnO. Banerjee *et al.*<sup>6</sup> reported the enhancement of ferromagnetism in pure ZnO powder upon thermal annealing, which was linked to the formation of oxygen vacancy ( $V_o$ ) clusters. Xu *et al.*<sup>7</sup> also reported ferromagnetism in ZnO thin films and attributed it to the intrinsic defects. Most recently, Potzger *et al.*<sup>8</sup> produced ferromagnetism in pure ZnO powder by applying mechanical force, where strain and domain boundaries were considered as the origin of the observed ferromagnetic signals.

So far, most of the previous magnetic studies on pure ZnO have been concentrated on bulk and thin film samples. However, there has been no systematic investigation on magnetic characteristics of undoped ZnO nanowires (NWs). With high surface-to-volume ratios, the electronic configuration of one-dimensional NWs is amenable to be altered, which could be used as a tool to establish long range magnetic ordering.<sup>9</sup> In this letter, we report a comparative study on the ferromagnetism in undoped single-crystalline ZnO NWs grown by the

vapor transport method. By carefully selecting the catalyst and varying the growth temperature, we can reproducibly tune the oxygen content in the NWs, which is accompanied by the characteristic defect-related emissions in the photoluminescence (PL) spectra. Our systematic studies suggest that both the PL and the RTFM are closely correlated with the oxygen deficiency in the undoped ZnO NWs.

Three types of ZnO NWs were prepared by using the vapor transport method in a horizontal tube furnace equipped with a gas supply and pumping system. The experimental setup was described in previous reports.<sup>10–13</sup> Typically, ZnO or Zn powder was used as the source, and argon mixed with 5% oxygen was used as the carrying gas. Silicon substrates were sputtered with 2 nm Au or Ag film as the catalyst before being placed downstream 5–6 cm away from the source. The experimental conditions and the properties of the synthesized NWs are summarized in Table I.

As shown in the scanning electron microscopy (SEM) images in Fig. 1(a), Au catalyst and a high growth temperature (960 °C) give randomly dispersed NWs (sample NW-1) with diameters of 50–100 nm and lengths of a few micrometers. On the other hand, a low temperature (520 °C) growth gives thicker and shorter NWs [Fig. 1(b), sample NW-2]. The Ag catalyzed sample grown at low temperature (sample NW-3) shows vertically aligned NWs [Fig. 1(c)]. In the x-ray diffraction (XRD) patterns [Fig. 1(d)], all peaks can be identified with the crystalline wurtzite ZnO structure. Except the catalyst Au in NW-1 and NW-2, there is no detectable secondary phase.

X-ray photoelectron spectroscopy (XPS) measurements were performed on these NW samples to assess the oxygen content. The survey scans show no impurity above the detection limit. Figures 1(e)–1(g) depict the multicomponent fitting to the O 1s peaks in NW-1, NW-2, and NW-3, respectively, which were normalized by the Zn 2p peaks

<sup>a)</sup>Author to whom correspondence should be addressed. Electronic mail: tomwu@ntu.edu.sg.

TABLE I. Growth conditions and experimental results of undoped ZnO NWs grown by the vapor transport method.

Sample	Source	Catalyst	Source temperature (°C)	Substrate temperature (°C)	Oxygen deficiency (%)	GB/UV emission ratio	$H_c$ at 5 K/RT (Oe)	$M_s$ at RT ( $\mu_B/V_O$ )
NW-1	ZnO/C	Au	960	850	20	62.58	190/115	0.0076
NW-2	Zn	Au	520	470	10	2.87	145/76	0.0030
NW-3	Zn	Ag	520	470	4	0.04	77/44	0.0003

accordingly. The peaks at lower and higher energies can be attributed to  $O^{2-}$  ions and absorbed oxygen, respectively.<sup>14</sup> The relative chemical compositions were calculated and we determined the nonstoichiometric formula for samples NW-1, NW-2, and NW-3 to be  $ZnO_{0.80}$ ,  $ZnO_{0.90}$ , and  $ZnO_{0.96}$ , respectively, and the corresponding O/Zn atomic ratios were plotted in Fig. 1(h). Previous theoretical calculations have suggested that the high oxygen deficiency in oxides should be attributed to oxygen vacancies instead of cation interstitials due to their lower formation energy.<sup>15</sup> Thus we can conclude that the concentrations of oxygen vacancies were systematically adjusted in these samples.

PL measurements were carried out by using a He-Cd laser with an excitation wavelength of 325 nm. In the PL spectra taken at RT [Fig. 2(a)], a near-band-edge (NBE) UV peak dominates in NW-3, but significantly weaker in NW-1. On the other hand, NW-1 is featured with a broad deep level emission (DLE) in the visible region, which can be ascribed to the transitions of the excited optical centers from the deep levels to the valence band.<sup>16</sup> These deep levels are associated with the intrinsic defects in the NWs, presumably oxygen vacancies. The integrated intensity ratio of the defect green emission to the UV emission (GB/UV) is largest in NW-1 and smallest in NW-3. Considering this strong contrast, we focus on the PL results obtained on these two samples. Figure 2(b) illustrates the low temperature (5 K) PL spectra for NW-1 and NW-3. The NBE emission dominates the PL spectra of NW-3, and as shown in Fig. 2(c), the associated fine structures were clearly resolved. The emission peaks at 3.365 and 3.360 eV can be assigned to excitons bound to neutral donors ( $D^0X$ )<sup>2,16</sup> and acceptor-bound excitons ( $A^0X$ ),<sup>2</sup> respectively. In Fig. 2(b) the peak located at 3.310 eV might be the first LO photon replica of the free exciton ( $1LO-FE_A^{n=1}$ ).<sup>2</sup> The  $D^0X$  NBE emission is much stronger in NW-1 than that

in NW-3 due to the presence of high-density oxygen vacancies as donors. In Fig. 2(b), DLE (green emission band) shows fine structures, which repeat with a longitudinal optical-phonon-energy spacing ( $\sim 72$  meV) and are associated with the transitions involving shallow donors (oxygen vacancies).<sup>17</sup> Fig. 2(d) shows the temperature-dependent PL spectra of NW-1, illustrating the evolution of the dominant DLE from RT down to 5 K.

The contrasts in oxygen content and optical characteristics in samples NW-1, NW-2, and NW-3 motivated us to carry out a comparative study on their magnetic properties. Magnetization measurements were carried out by using a superconducting quantum interference devices magnetometer (SQUID, Quantum Design, MPMSXL-5). Only plastic tweezers were used throughout the experiments to avoid unintentional metal contamination. The diamagnetic backgrounds of the Si substrates were subtracted from the raw data. Considering that nanoscale Au, Ag may induce weak ferromagnetism,<sup>18,19</sup> we first investigated the magnetic characteristics of the silicon substrates coated with Au or Ag thin films. All substrates without NWs growth showed only diamagnetic behaviors. Figure 3(a) depicts the magnetization versus magnetic field ( $M-H$ ) curves measured on NW-1, NW-2, and NW-3 at 5 and 300 K. Both NW-1 and NW-2 exhibit clear hysteresis loops, suggesting RTFM. In contrast, the magnetism is very weak in NW-3. Remarkably, the magnetization of NW-1 is about 25 times higher than that of NW-3. As shown in Fig. 3(b), the magnetizations versus temperature ( $M-T$ ) curves were measured under a magnetic field of 500 Oe under both zero-field-cooled (ZFC) and field-

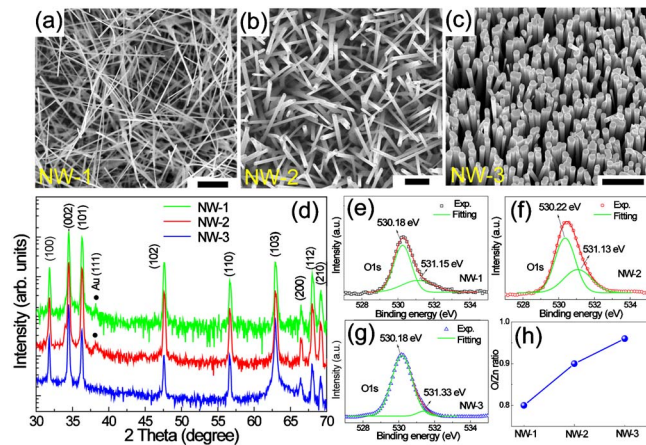


FIG. 1. (Color online) FESEM images of ZnO NWs in (a) NW-1, (b) NW-2, and (c) NW-3. The scale bars are 1  $\mu m$ . (d) Corresponding XRD patterns. [(e)-(g)] Normalized XPS O 1s scans. (h) O/Zn atomic ratios of three types of NWs.

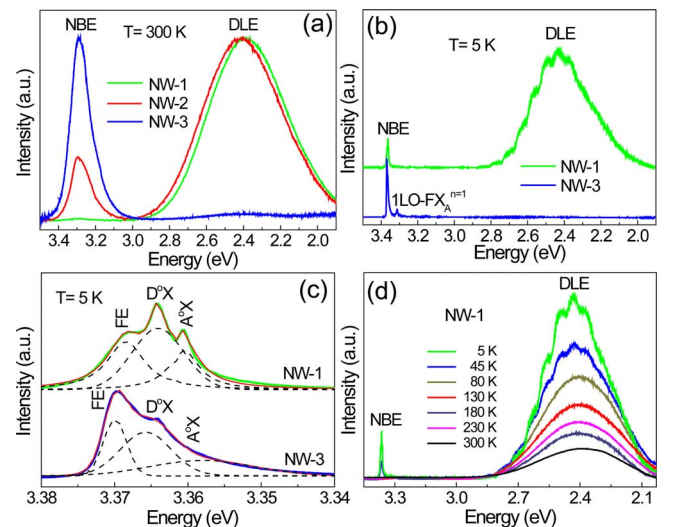


FIG. 2. (Color online) (a) RT PL spectra of NW-1, NW-2, and NW-3. (b) 5 K PL spectra of NW-1 and NW-3. (c) Enlarged view of the NBE region of NW-1 and NW-3 at 5 K. (d) Temperature-dependent PL spectra of NW-1 from 5 to 300 K.



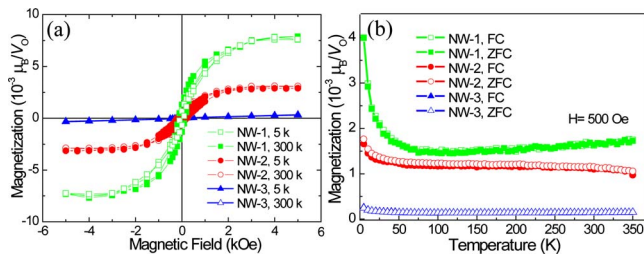


FIG. 3. (Color online) (a)  $M-H$  loops of NW-1, NW-2, and NW-3 taken at 5 and 300 K. (b) ZFC and FC temperature-dependent magnetization curves.

cooled (FC) conditions. In accordance with the  $M-H$  data, the temperature-dependent magnetization of NW-1 is much stronger than those of NW-2 and NW-3, which we attribute to the presence of substantial oxygen vacancies in NW-1.

A comparative study on these three kinds of NW samples revealed a strong correlation between the ferromagnetism and the oxygen deficiency. The RT saturation magnetizations and the GB/UV emission ratios of NW-1, NW-2, and NW-3 versus their corresponding levels of oxygen deficiency are shown in Fig. 4. The trend is clear: oxygen vacancies boost both the GB emission and the magnetism. However, it is noteworthy that the GB/UV emission ratio in NW-1 is more than twenty times higher than that in NW-2 while changes in the oxygen deficiency level and saturation magnetization are much more modest. This result indicates that a certain density of oxygen vacancies is needed in order to completely quench the NBE emission. Although both PL and magnetic properties are closely linked with the oxygen deficiency, the associated physical mechanisms and their quantitative dependence are very different.

RTFM has been observed previously in undoped wide band gap oxide thin films and nanoparticles such as  $\text{TiO}_2$ ,  $\text{HfO}_2$ ,  $\text{In}_2\text{O}_3$ ,  $\text{CeO}_2$ , and  $\text{SnO}_2$ , and its origin is usually linked to the oxygen deficiency.<sup>20,21</sup> These findings of RTFM with the absence of any transition metal doping have attracted significant attention and were called “ $d^0$  ferromagnetism.”<sup>22</sup> The RTFM in our samples can be attributed to the large population of bond defects, i.e.,  $V_o$ , since they can initiate defect-related hybridization at the Fermi level and establish a long-range ferromagnetic ordering.<sup>23</sup> A high concentration of  $V_o$  could also promote the probable formation of anionic vacancy clusters which can induce sizable magnetic moments.<sup>6</sup> Although our result does not exclude other types of defects like cation vacancies as the origin of long range ferromagnetic ordering,<sup>24,25</sup> these defects often have higher formation energy than  $V_o$  and can form only in oxygen rich environments.<sup>26</sup> Our experiments were carried out in oxygen poor conditions where  $V_o$  always contributes to the nonstoichiometry.<sup>27</sup> The tunable RTFM in NW samples confirms that oxygen vacancies can be purposely used to establish and regulate the ferromagnetic ordering.

In summary, we found that the concentration of oxygen vacancies directly regulates both the well-known defects-related green emission and the ferromagnetism. The present study not only demonstrates that undoped ZnO NWs can emit green light and show RTFM with energetic stability, but also suggests that introducing oxygen vacancies is an effective way to boost the  $d^0$  ferromagnetism. These engineered NWs with carefully tailored composition may find potential applications in nanoscale spintronic devices.

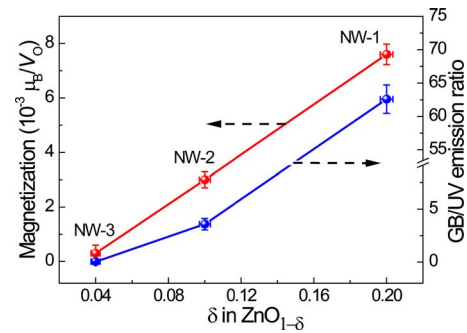


FIG. 4. (Color online) RT saturation magnetizations and GB/UV emission ratios of NW-1, NW-2, and NW-3 vs the corresponding oxygen deficiency levels.

This work was supported by the Singapore Ministry of Education Research Grant (Grant Nos. SUG 20/06 and RG 46/07). G. Z. Xing acknowledges financial support from Singapore Millennium Foundation, Singapore.

- <sup>1</sup>I. Žutić, J. Fabian, and S. Das Sarma, *Rev. Mod. Phys.* **76**, 323 (2004).
- <sup>2</sup>Ü. Özgür, Y. I. Alivov, C. Liu, A. Teke, M. A. Reshchikov, S. Dogan, V. Avrutin, S. J. Cho, and H. Morko, *J. Appl. Phys.* **98**, 041301 (2005).
- <sup>3</sup>K. Ando, H. Saito, Z. Jin, T. Fukumura, M. Kawasaki, Y. Matsumoto, and H. Koinuma, *J. Appl. Phys.* **89**, 7284 (2001).
- <sup>4</sup>A. Walsh, J. L. F. Da Silva, and S. H. Wei, *Phys. Rev. Lett.* **100**, 256401 (2008).
- <sup>5</sup>G. Z. Xing, J. B. Yi, J. G. Tao, T. Liu, L. M. Wong, Z. Zhang, G. P. Li, S. J. Wang, J. Ding, T. C. Sum, C. H. A. Huan, and T. Wu, *Adv. Mater. (Weinheim, Ger.)* **20**, 3521 (2008).
- <sup>6</sup>S. Banerjee, M. Mandal, N. Gayathri, and M. Sardar, *Appl. Phys. Lett.* **91**, 182501 (2007).
- <sup>7</sup>Q. Xu, H. Schmidt, S. Zhou, K. Potzger, M. Helm, H. Hochmuth, M. Lorenz, A. Setzer, P. Esquinazi, C. Meinelcke, and M. Grundmann, *Appl. Phys. Lett.* **92**, 082508 (2008).
- <sup>8</sup>K. Potzger, Z. Shengqiang, J. Grenzer, M. Helm, and J. Fassbender, *Appl. Phys. Lett.* **92**, 182504 (2008).
- <sup>9</sup>M. A. Garcia, J. M. Merino, E. F. Pinel, A. Quesada, J. de la Venta, M. L. R. Gonzalez, G. R. Castro, P. Crespo, J. Llopis, J. M. Gonzalez-Calbet, and A. Hernando, *Nano Lett.* **7**, 1489 (2007).
- <sup>10</sup>Z. Zhang, Y. H. Sun, Y. G. Zhao, G. P. Li, and T. Wu, *Appl. Phys. Lett.* **92**, 103113 (2008).
- <sup>11</sup>Z. Zhang, L. M. Wong, H. G. Ong, X. J. Wang, J. L. Wang, S. J. Wang, H. Y. Chen, and T. Wu, *Nano Lett.* **8**, 3205 (2008).
- <sup>12</sup>T. Chen, G. Z. Xing, Z. Zhang, H. Y. Chen, and T. Wu, *Nanotechnology* **19**, 435711 (2008).
- <sup>13</sup>G. Z. Xing, J. B. Yi, D. D. Wang, L. Liao, T. Yu, Z. X. Shen, C. H. A. Huan, T. C. Sum, J. Ding, and T. Wu, *Phys. Rev. B* **79**, 174406 (2009).
- <sup>14</sup>L. J. Meng, C. P. Moreira, and M. P. d. Santos, *Appl. Surf. Sci.* **78**, 57 (1994).
- <sup>15</sup>S. Lany and A. Zunger, *Phys. Rev. Lett.* **98**, 045501 (2007).
- <sup>16</sup>A. B. Djurišić, and Y. H. Leung, *Small* **2**, 944 (2006).
- <sup>17</sup>D. C. Reynolds, D. C. Look, and B. Jogai, *J. Appl. Phys.* **89**, 6189 (2001).
- <sup>18</sup>H. Hori, Y. Yamamoto, T. Iwamoto, T. Miura, T. Teranishi, and M. Miyake, *Phys. Rev. B* **69**, 174411 (2004).
- <sup>19</sup>L. Suber, D. Fiorani, G. Scavia, P. Imperatori, and W. R. Plunkett, *Chem. Mater.* **19**, 1509 (2007).
- <sup>20</sup>N. H. Hong, J. Sakai, N. Poirrot, and V. Brize, *Phys. Rev. B* **73**, 132404 (2006).
- <sup>21</sup>A. Sundaresan, R. Bhargavi, N. Rangarajan, U. Siddesh, and C. N. R. Rao, *Phys. Rev. B* **74**, 161306(R) (2006).
- <sup>22</sup>J. M. D. Coey, *Solid State Sci.* **7**, 660 (2005).
- <sup>23</sup>J. M. D. Coey, M. Venkatesan, and C. B. Fitzgerald, *Nature Mater.* **4**, 173 (2005).
- <sup>24</sup>I. S. Elifimov, S. Yunoki, and G. A. Sawatzky, *Phys. Rev. Lett.* **89**, 216403 (2002).
- <sup>25</sup>J. A. Chan, S. Lany, and A. Zunger, *Phys. Rev. Lett.* **103**, 016404 (2009).
- <sup>26</sup>F. Oba, S. R. Nishitani, S. Isotani, H. Adachi, and I. Tanaka, *J. Appl. Phys.* **90**, 824 (2001).
- <sup>27</sup>F. Oba, A. Togo, I. Tanaka, J. Paier, and G. Kresse, *Phys. Rev. B* **77**, 245202 (2008).